Vietnam Journal of Mechanics, Vol. 44, No. 4 (2022), pp. 514 – 525
DOI: https://doi.org/10.15625/0866-7136/17980

NONLINEAR BUCKLING AND POST-BUCKLING OF IMPERFECT FG POROUS SANDWICH CYLINDRICAL PANELS SUBJECTED TO AXIAL LOADING ON ELASTIC FOUNDATION

Pham Van Hoan[1], **Dao Nhu Mai**[2], **Khuc Van Phu**[1], **Le Kha Hoa**[1]
[1]*Military Academy of Logistics, Hanoi, Vietnam*
[2]*Institute of Mechanics, VAST, Hanoi, Vietnam*
*E-mail: lhoanhd@gmail.com

Received: 27 December 2022 / Published online: 31 December 2022

Abstract. This paper deals with the nonlinear buckling and post-buckling of sandwich cylindrical panels with non-uniform porous core and functionally graded face sheets. The imperfect sandwich cylindrical panels are subjected to axial loading on elastic foundation. Based on the Donnell shell theory, with von Kármán geometrical nonlinearity, the governing equations are derived. The effects of elastic foundation, various panel geometrical characteristics, porosity parameters, and the thickness of the porous core are investigated. The effects of foundation parameters, porosity parameters, the thickness of the porous core, and material parameters are investigated.

Keywords: analytical methods, FGP cylindrical panel, elastic foundation, nonlinear stability.

1. INTRODUCTION

Porous material has been known as a new type of lightweight material with mechanical properties that change continuously along the thickness of structures. The desired mechanical properties of this material can be achieved by adjusting the distribution law as well as the local density of pores in the structures. Possesses excellent energy-absorbing capability, functionally graded porous (FGP) materials has received wide application. Hence, numerous studies on the mechanical response of FGP structures have been widely implemented and reported. Using finite element analysis, Chen et al. [1] researched the dynamic response and energy absorption of FG porous structures. Using Ritz method, Chen and his coworkers [2–4] studied elastic buckling, static bending, and vibrations of FGP beam. The important research on the static and dynamic of FGP plates are given by Magnucki and his co-workers [5], Rezaei and Saidi [6], Tu et al. [7]. With FGP shells, Thai et al. [8], Nam et al. [9], and Foroutan and his co-workers [10] applied the

Galerkin method to study the nonlinear stability of FGP conical shells and FGP cylinders under axial loading, torsion and hygrothermal loading.

Cylindrical panels are used as common structural load-bearing components in modern engineering. The buckling and post-buckling response are important mechanical characteristics of the composite cylindrical panel and have attracted many researchers. Using singular perturbation techniques, Shen [11] presented the post-buckling of FGM cylindrical panels under axial load in thermal environments. Based on Rayleigh–Ritz method, an assessment of shell theories for buckling of composite laminated cylindrical panels under axial loading is presented by Jaunky and Knight [12]. Based on Karman–Donnell's theory, Duc and Tung [13], Dung and Hoa [14] studied thermo-mechanical post-buckling behavior of FGM cylindrical panels subjected to axial loading without and with temperature-dependent properties. Therein, Poisson's ratio is considered to depend on the thickness z.

There are many authors studied cylindrical panels resting on elastic foundations. Based on Timoshenko-Mindlin kinematic hypotheses and Hamilton's principle, Fu and Chia [15] analyzed nonlinear of unsymmetrically laminated imperfect thick panels on elastic foundation. Turvey [16] investigated the buckling of cylindrical panels on elastic foundations with simply supported boundary conditions. Based on the dynamic Marguerre-type equations, Chia [17] studied nonlinear vibration and postbuckling of unsymmetrically laminated imperfect shallow cylindrical panels with mixed boundary conditions resting on elastic foundation. The Galerkin procedure furnishes an equation for the time function which is solved by the method of perturbation. Based on the Reddy's third order shear deformation shell theory and using a singular perturbation technique along with a two-step perturbation approach, Shen and Xiang [18] researched the effect of negative Poisson's ratio on the axially compressed postbuckling behavior of FG-GRMMC laminated cylindrical panels on elastic foundations in thermal environments. Based on Galerkin's method, Duc et al. [19–21] presented nonlinear static, dynamic and vibration of imperfect ES-FGM cylindrical shells on elastic foundation. With the same method, Trang and Tung [22] analyzed the nonlinear responses of composite cylindrical panels reinforced by single-walled carbon nanotubes, supported by an elastic foundation, exposed to elevated temperature and axially compressed by uniform load.

However, the problem of the nonlinear analysis of FG porous cylindrical panels subjected to mechanical or thermal loading is restricted. Recently, the results on the nonlinear vibration of FGP porous cylindrical panels have been considered by Keleshteri and Jelovica [23], Akbari et al. [24], Anh and Duc [25]. Using the Galerkin method, Do Quang Chan and the authors [26] studied the nonlinear stability of imperfect cylindrical panels made of FGP sandwich materials subjected to axial compression with different boundary conditions. The studied FGP sandwich panel consists of three layers, in which the two outer layers are made of variable mechanical properties and the middle layer is made of symmetrical porous materials. The numerical results show the influence of geometrical parameters, porosity parameter e_0, and foam core layer thickness on the buckling and

post-buckling of the FG porous sandwich cylindrical panel. Developing the article [26], this study analyzes the influence of the foundation coefficients on the nonlinear stability of the imperfect FGP sandwich cylindrical panel under axial compression. The sandwich cylindrical panel considered is composed of symmetric porous core and FG face sheets subjected to axial loads. The material properties of the two face sheets are assumed to be continuously graded in the thickness direction according to a simple power-law distribution in terms of the volume fraction of constituents. The core layer is made of symmetric porous material characterized by a porosity coefficient which influences the physical properties of the panel in the form of the simple cosine function in the panel thickness direction. The material continuity of face sheets-core and face sheets-stiffeners is guaranteed. Based on the Donnell shell theory, the Galerkin method are applied to solve the nonlinear problem.

2. FG POROUS SANDWICH CYLINDRICAL PANELS

In this study, a symmetric porous sandwich cylindrical panel with FG coating and the cylindrical coordinate system with axes x, y, z depicted in Fig. 1 is examined. Where R, a, b are mean radius, length of straight edge, and curved edge, respectively. The thickness of each FG coating layer and porous layer are $h_{FG}/2$ and h_{core}. The total thickness of FG porous sandwich panels is h ($h = h_{core} + h_{FG}$).

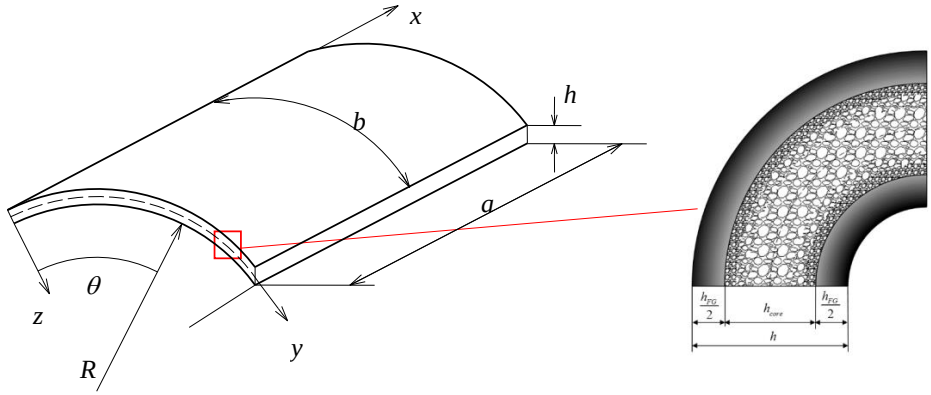

Fig. 1. Geometry of symmetric porous cylindrical panels with FG coating

Young moduli and Poisson's ratios of shell is determined

$$(E_{sh}, \nu_{sh}) = \begin{cases} (E_c, \nu_c) + (E_{mc}, \nu_{mc}) \left(\dfrac{2z + h_{FG} + h_{core}}{h_{FG}} \right)^p & -\dfrac{h_{FG} + h_{core}}{2} < z < -\dfrac{h_{core}}{2} \\ (E_m, \nu_m) \left[1 - e_0 \cos \left(\dfrac{\pi z}{h_{core}} \right) \right] & -\dfrac{h_{core}}{2} < z < \dfrac{h_{core}}{2} \\ (E_c, \nu_c) + (E_{mc}, \nu_{mc}) \left(\dfrac{-2z + h_{FG} + h_{core}}{h_{FG}} \right)^p & \dfrac{h_{core}}{2} < z < \dfrac{h_{FG} + h_{core}}{2} \end{cases} \tag{1}$$

$$E_{mc} = E_m - E_c, \nu_{mc} = \nu_m - \nu_c,\ p \geq 0.$$

The notation c, m and sh denote ceramic, metal and shell, respectively. p is the volume fraction index of the two functionally graded layers of the panel. The porosity coefficient is e_0 $(0 \leq e_0 < 1)$. Young's modulus of the metal, ceramic and shell are E_m, E_c, E_{sh}. Poisson's ratios of the metal and ceramic are ν_m, ν_c, ν_{sh}, respectively.

3. NONLINEAR EQUILIBRIUM EQUATIONS TAKING INTO ACCOUNT ELASTIC FOUNDATION EFFECT

Based on the Donnell shell theory with von Karman geometrical nonlinearity, the nonlinear equilibrium equations of imperfect FGP cylindrical panel, taking into account a two-parameter elastic foundation are given by [19–22]

$$\begin{aligned} A_3\nabla^4 f + \frac{1}{R}f_{,xx} + A_4\nabla^4 w + f_{,yy}\left(w_{,xx} + w^*_{,xx}\right) - 2f_{,xy}\left(w_{,xy} + w^*_{,xy}\right) \\ + f_{,xx}\left(w_{,yy} + w^*_{,yy}\right) + K_s(w_{,xx} + w_{,yy}) - K_w w = 0, \end{aligned} \tag{2}$$

$$\nabla^4 f + A_1\nabla^4 w - A_2\left(w^2_{,xy} - w_{,xx}w_{,yy} - w_{,xx}/R + 2w_{,xy}w^*_{,xy} - w_{,xx}w^*_{,yy} - w_{,yy}w^*_{,xx}\right) = 0, \tag{3}$$

where w is the displacement components of the mid-plane of the plate in z-direction, the quantity $w*$ is an initial imperfection of porous panel, $f(x, y)$ is the Airy stress function and K_w, K_s are foundation parameters

$$A_1 = J_2/D_{11},\ A_2 = 1/\left(J_0 D_{11}\right), \quad A_3 = J_0 J_2, \quad A_4 = J_0\left(D_{12}J_1 + D_{22}J_2\right) - D_{13},$$

$$J_0 = \frac{1}{D_{11}^2 - D_{21}^2}, \quad J_1 = D_{11}D_{12} - D_{21}D_{22}, \quad J_2 = D_{11}D_{22} - D_{21}D_{12}.$$

with

$$D_{11} = \frac{E_1}{1-\nu^2}, \quad D_{12} = \frac{E_2}{1-\nu^2}, \quad D_{13} = \frac{E_3}{1-\nu^2}, \quad E_1 = \int_{-h/2}^{h/2} E_{sh}\mathrm{d}z,$$

$$D_{21} = \frac{\nu E_1}{1-\nu^2}, \quad D_{22} = \frac{\nu E_2}{1-\nu^2}, \quad D_{23} = \frac{\nu E_3}{1-\nu^2}, \quad E_2 = \int_{-h/2}^{h/2} zE_{sh}\mathrm{d}z,$$

$$D_{31} = \frac{E_1}{2\left(1+\nu\right)}, \quad D_{32} = \frac{E_2}{2\left(1+\nu\right)}, \quad D_{33} = \frac{E_3}{2\left(1+\nu\right)}, \quad E_3 = \int_{-h/2}^{h/2} z^2 E_{sh}\mathrm{d}z.$$

Assume four edges are simply supported

$$\begin{aligned} w = M_x = N_{xy} = 0,\ N_x = -r_0 h \quad \text{at } x = 0,\ x = a, \\ w = M_y = N_{xy} = 0,\ N_y = -p_0 h \quad \text{at } y = 0,\ y = b. \end{aligned} \tag{4}$$

According to Eqs. (4), the w function are chosen as [20,22,26]

$$\begin{aligned} w &= W \sin \alpha x \sin \beta y, \\ w^* &= W^* \sin \alpha x \sin \beta y. \end{aligned} \tag{5}$$

where $\alpha = \dfrac{m\pi}{a}; \beta = \dfrac{n\pi}{b}; W^* = \xi h; 0 \le \xi \le 1; m, n = 1, 2, 3, \ldots$

Substituting Eq. (5) into Eq. (3), the solution of the equation is [20,22]

$$f = B_1 \cos 2\alpha x + B_2 \cos 2\beta y + B_3 \sin \alpha x \sin \beta y + \frac{1}{2} N_x y^2 + \frac{1}{2} N_y x^2 \tag{6}$$

where $B_1 = \dfrac{A_2(W^2\beta^2 + 2WW^*\beta^2)}{32\alpha^2}; B_2 = \dfrac{A_2(W^2\alpha^2 + 2WW^*\alpha^2)}{32\beta^2}; B_3 = \dfrac{A_2 W \alpha^2}{R(\alpha^2+\beta^2)^2} - A_1 W.$

Substituting Eqs. (5), (6) into Eq. (2) then using Galerkin method, yields

$$\begin{aligned} & W\left[\left(A_3(\alpha^2+\beta^2)^2 - \frac{\alpha^2}{R}\right)\left(\frac{A_2\alpha^2}{R(\alpha^2+\beta^2)^2} - A_1\right) + A_4(\alpha^2+\beta^2)^2\right]\frac{1}{4} \\ & + (W^2 + 2W^*W)\left[-4A_2A_3\alpha^2\beta^2 + \frac{A_2\beta^2}{2R}\right]\frac{\delta_1\delta_2}{3mn\pi^2} \\ & + W(W^* + W)\left(\frac{A_2\alpha^2}{R(\alpha^2+\beta^2)^2} - A_1\right)\frac{8\alpha^2\beta^2}{3mn\pi^2}\delta_1\delta_2 \\ & - (W^* + W)(W^2 + 2W^*W)\frac{A_2\left(\alpha^4+\beta^4\right)}{64} - \frac{1}{4}\left[K_s\left(\alpha^2+\beta^2\right) + K_w\right]W \\ & = (W^* + W)\frac{1}{4}\left(N_x\alpha^2 + N_y\beta^2\right) - \frac{N_y}{R}\frac{4}{mn\pi^2}\delta_1\delta_2 \end{aligned}$$

$$\begin{aligned} \Leftrightarrow\ & S_1 W + S_2(W^2 + 2W^*W) + S_3 W(W^* + W) - S_4(W^* + W)(W^2 + 2W^*W) \\ & - \frac{1}{4}\left[K_s\left(\alpha^2+\beta^2\right) + K_w\right]W = (W^* + W)\frac{1}{4}\left(N_x\alpha^2 + N_y\beta^2\right) - \frac{N_y}{R}\frac{4}{mn\pi^2}\delta_1\delta_2, \end{aligned} \tag{7}$$

where

$$\begin{aligned} \delta_1 &= \frac{1}{2}\left[1 - (-1)^m\right], \quad \delta_2 = \frac{1}{2}\left[1 - (-1)^n\right], \\ S_1 &= \left[\left(A_3(\alpha^2+\beta^2)^2 - \frac{\alpha^2}{R}\right)\left(\frac{A_2\alpha^2}{R(\alpha^2+\beta^2)^2} - A_1\right) + A_4(\alpha^2+\beta^2)^2\right]\frac{1}{4}, \\ S_2 &= \left[-4A_2A_3\alpha^2\beta^2 + \frac{A_2\beta^2}{2R}\right]\frac{1}{3mn\pi^2}\delta_1\delta_2, \\ S_3 &= \left(\frac{A_2\alpha^2}{R(\alpha^2+\beta^2)^2} - A_1\right)\frac{8\alpha^2\beta^2}{3mn\pi^2}\delta_1\delta_2; S_4 = \frac{A_2\left(\alpha^4+\beta^4\right)}{64}. \end{aligned}$$

Consider FG porous sandwich cylindrical panel subjected to axial loading on elastic foundation, taking $N_{x0} = -r_0 h, N_{y0} = -p_0 h = 0$, Eq. (7) yields

$$r_0 = \frac{-4}{h\alpha^2(W^* + W)} \left\{ \begin{array}{l} S_1 W + S_2 W(W + 2W^*) + S_3 W(W^* + W) \\ -S_4 W(W^* + W)(W + 2W^*) - \frac{1}{4}\left[K_s\left(\alpha^2 + \beta^2\right) + K_w\right] W \end{array} \right\} \tag{8}$$

Using Eq. (8), the effects of foundation parameters, porosity parameters, the thickness of the porous core, and material parameters on post-buckling load-deflection can be analyzed.

For perfect FG porous sandwich cylindrical panel ($\xi = 0$), Eq. (8) leads to

$$r_0 = \frac{-4}{h\alpha^2}\left(S_1 + S_2 W + S_3 W - S_4 W^2 - \frac{1}{4}\left[K_s\left(\alpha^2 + \beta^2\right) + K_w\right]\right). \tag{9}$$

The upper buckling load of perfect cylindrical panels (buckled in bifurcation type) can be obtained when $W \to 0$ as

$$r_{0upper} = \frac{-4}{h\alpha^2}\left\{S_1 - \frac{1}{4}\left[K_s\left(\alpha^2 + \beta^2\right) + K_w\right]\right\}. \tag{10}$$

When not counting the elastic background ($K_w = K_s = 0$)

$$r_{0upper} = \frac{-4S_1}{h\alpha^2} = \frac{-1}{h\alpha^2}\left[\left(A_3(\alpha^2 + \beta^2)^2 - \frac{\alpha^2}{R}\right)\left(\frac{A_2\alpha^2}{R(\alpha^2 + \beta^2)^2} - A_1\right) + A_4(\alpha^2 + \beta^2)^2\right]. \tag{11}$$

The Eq. (11) is used the buckling load of the imperfect FGP sandwich cylindrical panel under axial compression.

4. NUMERICAL RESULTS

4.1. Comparisons

In this subsection, to validate the present method, the comparison is made for isotropic cylindrical panels under axial uniform load with simply supported four edges. Based on Eq. (11), Table 1 compares the buckling load of isotropic cylindrical panels under axial loading with the results given by Jaunky [12] and Shen [11]. Here in, the buckling load

Table 1. Comparisons of upper load N_{cr} of isotropic cylindrical panels under axial uniform loading: $E = 10^7$ psi, $\nu = 0.3$ and $h = 0.24$ in

a/b	a/R	b/h	Jaunky [12]		Shen [11]	Present
			FEM	Donnell-theory	HSDT	Donnell-theory
3.1831	10	78.5398	41945.4	53080.6	51419.68	53572.203 (8,4)*
3.1831	10	157.0796	12360.0	13834.1	13119.99	13378.790 (13,6)
3.1831	10	314.1593	3358.8	3549.9	3228.12	3344.882 (15,8)

*buckling mode (m, n).

$N_{cr} = r_{upper}/(bh)$ and r_{upper} is calculated by the Eq. (11). According to Table 1, it can conclude that the numerical solutions of this research are reliable.

4.2. FG porous sandwich cylindrical panels

The purpose of this work is to study the effects of foundation parameters, porosity parameters, the thickness of the porous core, and material parameters on the nonlinear buckling and post-buckling of sandwich cylindrical panels with non-uniform porous core and functionally graded face sheets. In the following sections, the cylindrical panel with two FGM face sheets between a metal foam core is considered. The FGM of face sheets and stiffeners are mixture of Zirconia (ceramic) and Ti-6Al-4V (metal). The core layer made of metal foam is Ti-6Al-4V and Poisson's ratio $v = 0.3$. The volume fraction indexes, geometrical parameters of panels, porosity coefficients and foundation parameters are taken as: $p = 1, h = 0.006$ m, $a/b = 1.5, b/h = 50, a/R = 0.5, h_{core}/h_{FG} = 5, e_0 = 0.5$, $K_w = 6 \times 10^7$ N/m^3, $K_s = 5 \times 10^5$ N/m.

Table 2. Influence of foundation parameters (K_w, K_s) on upper critical loads (r_{upper}) $p = 1, h = 0.006$ m, $a/b = 1.5, b/h = 50, a/R = 0.5, \xi = 0, h_{core}/h_{FG} = 5$

K_w (N/m^3)	K_s (N/m)	r_{upper} (MPa)			
		$e = 0$	$e = 0.2$	$e = 0.5$	$e = 0.8$
$K_w = 0$	$K_s = 0$	468.9710 (1,1)*	434.5646 (1,1)	382.9550 (1,1)	331.2172 (2,1)
$K_w = 3 \times 10^7$	$K_s = 0$	481.4556 (3,1)	451.2540 (3,1)	405.9517 (3,1)	356.8641 (2,1)
$K_w = 6 \times 10^7$	$K_s = 0$	492.8542 (3,1)	462.6527 (3,1)	417.3503 (3,1)	372.0480 (3,1)
$K_w = 9 \times 10^7$	$K_s = 0$	504.2529 (3,1)	474.0513 (3,1)	428.7489 (3,1)	383.4466 (3,1)
$K_w = 3 \times 10^7$	$K_s = 2 \times 10^5$	523.1223 (3,1)	492.9207 (3,1)	447.6183 (3,1)	402.3160 (3,1)
$K_w = 6 \times 10^7$	$K_s = 2 \times 10^5$	534.5209 (3,1)	504.3193 (3,1)	459.0170 (3,1)	413.7146 (3,1)
$K_w = 9 \times 10^7$	$K_s = 2 \times 10^5$	545.9195 (3,1)	515.7180 (3,1)	470.4156 (3,1)	425.1133 (3,1)
$K_w = 3 \times 10^7$	$K_s = 4 \times 10^5$	564.7889 (3,1)	534.5874 (3,1)	489.2850 (3,1)	443.9827 (3,1)
$K_w = 6 \times 10^7$	$K_s = 4 \times 10^5$	576.1876 (3,1)	545.9860 (3,1)	500.6836 (3,1)	455.3813 (3,1)
$K_w = 9 \times 10^7$	$K_s = 4 \times 10^5$	587.5862 (3,1)	557.3846 (3,1)	512.0823 (3,1)	466.7799 (3,1)
$K_w = 3 \times 10^7$	$K_s = 8 \times 10^5$	648.1223 (3,1)	617.9207 (3,1)	572.6183 (3,1)	527.3160 (3,1)
$K_w = 6 \times 10^7$	$K_s = 8 \times 10^5$	659.5209(3,1)	629.3193(3,1)	584.0170(3,1)	538.7146(3,1)
$K_w = 9 \times 10^7$	$K_s = 8 \times 10^5$	670.9195 (3,1)	640.7180 (3,1)	595.4156 (3,1)	550.1133 (3,1)

*buckling mode (m, n).

Table 2 shows the influence of foundation parameters (K_w, K_s) on upper critical loads (r_{upper}) of porous cylindrical panels with functionally graded composite coating. Figs. 2 and 3 describe the influence of the foundation parameters and the imperfections of the FGP cylindrical panel on the curve describing the axial compression load relationship with the deflection ratio W/h. Looking at Table 2, it can see that the upper axial load increase when the foundation coefficients increases. For example, with $e_0 = 0.5$, the

upper axial load increase about 55% from $r_{upper} = 382.9550$ MPa (with $K_w = K_s = 0$) to $r_{upper} = 595.4156$ MPa (with $K_w = 9 \times 10^7$ N/m^3, $K_s = 8 \times 10^5$ N/m). This problem also shown in Fig. 3 when using Eqs. (8) to describe the influence of the foundation coefficients on $r_0 - W/h$ curves. Fig. 2 shows the postbuckling load-deflection curves of perfect and imperfect porous panels. It can be seen that, the curves of imperfect porous panels start at original coordinates and the curves of perfect porous panels start at a point on the vertical axis of coordinates that means the deflection of the perfect porous panels only appears when the axial compression load is large enough – buckling load.

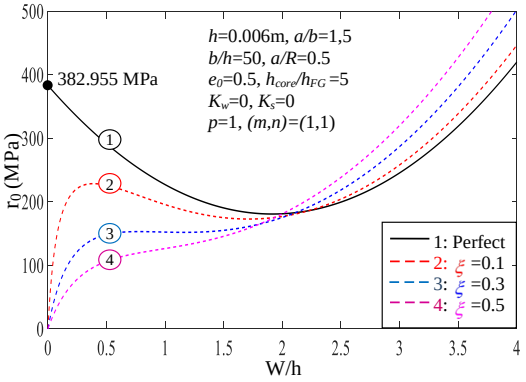

Fig. 2. Influence of ξ on $r_0 - W/h$ curves

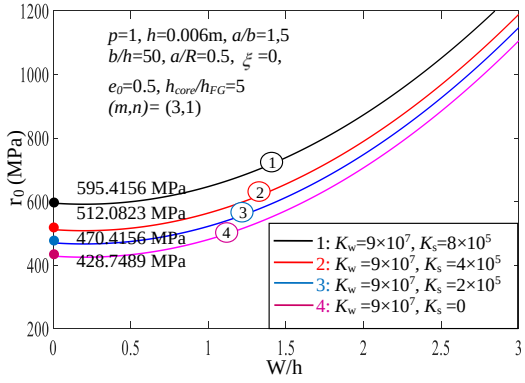

Fig. 3. Influence of K_w and K_s on $r_0 - W/h$ curves

Table 3. Influence of porosity coefficients e_0 and core layerh_{core}/h_{FG} on upper critical loads $p = 1, h = 0.006$ m, $a/b = 1.5, b/h = 50, a/R = 0.5, \xi = 0, K_w = 6 \times 10^7$ N/m^3, $K_s = 5 \times 10^5$ N/m

r_{upper} (MPa)	$e_0 = 0$	$e_0 = 0.2$	$e_0 = 0.5$	$e_0 = 0.8$
$h_{core}/h_{FG} = 0$	718.0359 (3,1)	718.0359 (3,1)	718.0359 (3,1)	718.0359 (3,1)
$h_{core}/h_{FG} = 1$	659.1270 (3,1)	644.8462 (3,1)	623.4251 (3,1)	602.0040 (3,1)
$h_{core}/h_{FG} = 3$	614.8104 (3,1)	589.3391 (3,1)	551.1321 (3,1)	512.9251 (3,1)
$h_{core}/h_{FG} = 5$	597.0209 (3,1)	566.8193 (3,1)	521.5170 (3,1)	476.2146 (3,1)
$h_{core}/h_{FG} = 10$	579.3658 (3,1)	544.3449 (3,1)	491.8136 (3,1)	439.2822 (3,1)
$h_{core} = h, h_{FG} = 0$	556.1821 (3,1)	514.6600 (3,1)	452.3767 (3,1)	390.0935 (3,1)

Based on Eq. (10), the influence of the thickness ratios of core layer-to-face layer (h_{core}/h_{FG}) and porosity coefficients e_0 on upper axial loads are shown in Table 3. Look at these number result, it can see that the upper axial load decreases about 59% from $r_{upper} = 718.0359$ MPa (with $h_{core}/h_{FG} = 0, e_0 = 0.5$) to $r_{upper} = 452.3767$ MPa (with $h_{core} = h, h_{FG} = 0, e_0 = 0.5$). Table 3 shows that the critical axial load decreases when porosity coefficients e_0 increases. For example, with $h_{core}/h_{FG} = 5$, the upper axial load decreases about 25% from $r_{upper} = 597.0209$ MPa (with $e_0 = 0$) to $r_{upper} = 476.2146$ MPa (with $e_0 = 0.8$). This proves that as the porosity of the cylindrical panel increases, the

bearing capacity of the panel becomes weaker. Thus, it can be concluded that the porosity coefficients e_0 and the thickness ratios of core layer-to-face layer h_{core}/h_{FG} has a significant effect on the compressive load capacity of porous panels. This problem also shown in Fig. 4 and Fig. 5 when using Eqs. (8) to describe the influence of the thickness ratios of core layer-to-face layer (h_{core}/h_{FG}) and porosity coefficients e_0 on $r_0 - W/h$ curves.

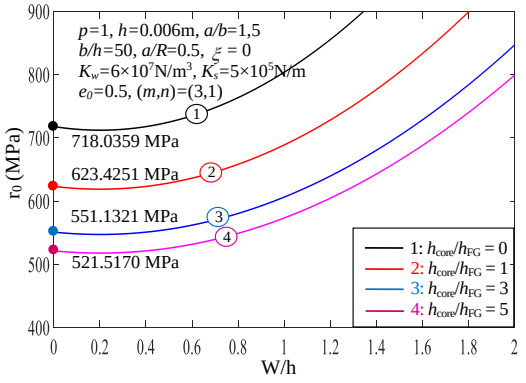

Fig. 4. Influence of h_{core}/h_{FG} on $r_0 - W/h$ curves

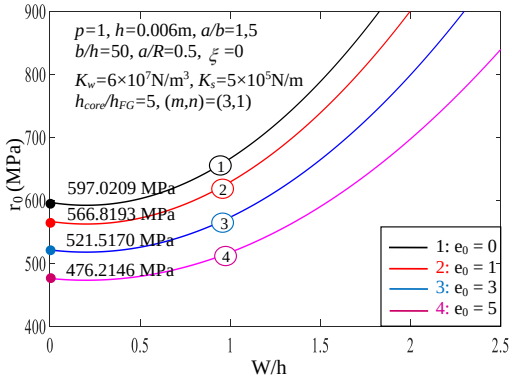

Fig. 5. Influence of e_0 on $r_0 - W/h$ curves

The effects of geometrical ratios a/b and a/R on critical axial load are shown in Table 4. The obtained results show that the upper axial load decreases as the a/b ratio increases and the upper axial load increases as the a/R ratio increases. For example, with the ratio $a/b = 2$ the upper limit load increases from $r_{upper} = 363.0327$ MPa with $a/R = 0.2$ to $r_{upper} = 587.1866$ MPa with $a/R = 0.8$ (about 62% increase) i.e. cylindrical panel the longer it is the lower the bearing capacity.

Table 4. Influence of a/b and a/R on upper critical loads (r_{upper}) $p = 1, h = 0.006$ m, $b/h = 50, h_{core}/h_{FG} = 5, \xi = 0, e_0 = 0.5, K_s = 5 \times 10^5$ N/m, $K_w = 6 \times 10^7$ N/m^3

r_{upper} (MPa)	$a/R = 0.2$	$a/R = 0.4$	$a/R = 0.5$	$a/R = 0.6$	$a/R = 0.8$
$a/b = 0.5$	587.1866 (1,1)	1100.6347 (2,1)	1267.9590 (2,1)	1472.4665 (2,1)	1950.7567 (2,2)
$a/b = 1$	425.9975 (2,1)	587.1866 (2,1)	708.0784 (2,1)	810.8271 (3,1)	1022.3878 (3,1)
$a/b = 1.5$	386.2391 (2,1)	467.7873 (3,1)	521.5170 (3,1)	587.1866 (3,1)	729.1057 (4,1)
$a/b = 2$	363.0327 (3,1)	416.6829 (3,1)	456.2205 (4,1)	493.1596 (4,1)	587.1866 (4,1)
$a/b = 3$	355.0744 (5,1)	376.8615 (5,1)	393.2017 (5,1)	413.1732 (5,1)	464.0095 (5,1)
$a/b = 4$	349.6202 (6,1)	363.0327 (6,1)	373.0921 (6,1)	385.3870 (6,1)	414.1460 (7,1)
$a/b = 5$	348.5246 (8,1)	356.6645 (8,1)	362.7693 (8,1)	370.2309 (8,1)	389.2238 (8,1)

5. CONCLUSIONS

Applying the Galerkin procedure with regard to the von Kármán nonlinearity, the nonlinear stability of imperfect FG porous sandwich cylindrical panels under axial compression on elastic foundation is analyzed in this paper. The sandwich cylindrical panels consist of metal foam core and FGM face-sheets. The accuracy of the existing solutions is verified by comparing with published data. The effects of foundation parameters, porosity parameters, the thickness of the porous core, and material parameters on the nonlinear buckling and post-buckling behavior are investigated. The results show the load-carrying capability of the FG porous cylindrical sandwich panel is increased when the foundation coefficients and geometrical ratio a/R increase. It will be decreased when porosity coefficients e_0, the thickness ratios of core layer-to-face layer h_{core}/h_{FG} and the geometrical ratio a/b increase. It is hoped that analyses presented in this paper will have significant contributions to accurate predictions and reliable design of FG porous sandwich cylindrical panels.

DECLARATION OF COMPETING INTEREST

The authors declare that they have no known competing financial interests or personal relationships that could have appeared to influence the work reported in this paper.

FUNDING

This research received no specific grant from any funding agency in the public, commercial, or not-for-profit sectors.

REFERENCES

[1] D. Chen, S. Kitipornchai, and J. Yang. Dynamic response and energy absorption of functionally graded porous structures. *Materials & Design*, **140**, (2018), pp. 473–487. https://doi.org/10.1016/j.matdes.2017.12.019.

[2] D. Chen, J. Yang, and S. Kitipornchai. Elastic buckling and static bending of shear deformable functionally graded porous beam. *Composite Structures*, **133**, (2015), pp. 54–61. https://doi.org/10.1016/j.compstruct.2015.07.052.

[3] D. Chen, J. Yang, and S. Kitipornchai. Free and forced vibrations of shear deformable functionally graded porous beams. *International Journal of Mechanical Sciences*, **108-109**, (2016), pp. 14–22. https://doi.org/10.1016/j.ijmecsci.2016.01.025.

[4] D. Chen, S. Kitipornchai, and J. Yang. Nonlinear free vibration of shear deformable sandwich beam with a functionally graded porous core. *Thin-Walled Structures*, **107**, (2016), pp. 39–48. https://doi.org/10.1016/j.tws.2016.05.025.

[5] K. Magnucki, M. Malinowski, and J. Kasprzak. Bending and buckling of a rectangular porous plate. *Steel and Composite Structures*, **6**, (4), (2006), pp. 319–333. https://doi.org/10.12989/scs.2006.6.4.319.

[6] A. S. Rezaei and A. R. Saidi. Exact solution for free vibration of thick rectangular plates made of porous materials. *Composite Structures*, **134**, (2015), pp. 1051–1060. https://doi.org/10.1016/j.compstruct.2015.08.125.

[7] T. M. Tu, L. K. Hoa, D. X. Hung, and L. T. Hai. Nonlinear buckling and post-buckling analysis of imperfect porous plates under mechanical loads. *Journal of Sandwich Structures & Materials*, **22**, (2018), pp. 1910–1930. https://doi.org/10.1177/1099636218789612.

[8] D.-K. Thai, T. M. Tu, L. K. Hoa, D. X. Hung, and N. N. Linh. Nonlinear stability analysis of eccentrically stiffened functionally graded truncated conical sandwich shells with porosity. *Materials*, **11**, (2018). https://doi.org/10.3390/ma11112200.

[9] V. H. Nam, N.-T. Trung, and L. K. Hoa. Buckling and postbuckling of porous cylindrical shells with functionally graded composite coating under torsion in thermal environment. *Thin-Walled Structures*, **144**, (2019). https://doi.org/10.1016/j.tws.2019.106253.

[10] K. Foroutan, A. Shaterzadeh, and H. Ahmadi. Nonlinear static and dynamic hygrothermal buckling analysis of imperfect functionally graded porous cylindrical shells. *Applied Mathematical Modelling*, **77**, (2020), pp. 539–553. https://doi.org/10.1016/j.apm.2019.07.062.

[11] H.-S. Shen. Postbuckling analysis of axially loaded functionally graded cylindrical panels in thermal environments. *International Journal of Solids and Structures*, **39**, (2002), pp. 5991–6010. https://doi.org/10.1016/s0020-7683(02)00479-1.

[12] N. Jaunky and N. F. K. Jr. An assessment of shell theories for buckling ofcircular cylindrical laminated composite panels loaded inaxial compression. *International Journal of Solids and Structures*, **36**, (1999), pp. 3799–3820. https://doi.org/10.1016/s0020-7683(98)00177-2.

[13] N. D. Duc and H. V. Tung. Nonlinear analysis of stability for functionally graded cylindrical panels under axial compression. *Computational Materials Science*, **49**, (2010), pp. S313–S316. https://doi.org/10.1016/j.commatsci.2009.12.030.

[14] D. V. Dung and L. K. Hoa. Nonlinear analysis of buckling and postbuckling for axially compressed functionally graded cylindrical panels with the Poisson's ratio varying smoothly along the thickness. *Vietnam Journal of Mechanics*, **34**, (2012), pp. 27–44. https://doi.org/10.15625/0866-7136/34/1/426.

[15] Y. M. Fu and C. Y. Chia. Nonlinear analysis of unsymmetrically laminated imperfect thick panels on elastic foundation. *Composite Structures*, **13**, (1989), pp. 289–314. https://doi.org/10.1016/0263-8223(89)90013-5.

[16] G. J. Turvey. Buckling of simply supported cross-ply cylindrical panels on elastic foundations. *The Aeronautical Journal*, **81**, (1977), pp. 88–91. https://doi.org/10.1017/s000192400003236x.

[17] C.-Y. Chia. Nonlinear vibration and postbuckling of unsymmetrically laminated imperfect shallow cylindrical panels with mixed boundary conditions resting on elastic foundation. *International Journal of Engineering Science*, **25**, (1987), pp. 427–441. https://doi.org/10.1016/0020-7225(87)90069-3.

[18] H.-S. Shen and Y. Xiang. Effect of negative Poisson's ratio on the axially compressed postbuckling behavior of FG-GRMMC laminated cylindrical panels on elastic foundations. *Thin-Walled Structures*, **157**, (2020). https://doi.org/10.1016/j.tws.2020.107090.

[19] N. D. Duc and T. Q. Quan. Nonlinear response of imperfect eccentrically stiffened FGM cylindrical panels on elastic foundation subjected to mechanical loads. *European Journal of Mechanics - A/Solids*, **46**, (2014), pp. 60–71. https://doi.org/10.1016/j.euromechsol.2014.02.005.

[20] N. D. Duc, N. D. Tuan, T. Q. Quan, N. V. Quyen, and T. V. Anh. Nonlinear mechanical, thermal and thermo-mechanical postbuckling of imperfect eccentrically stiffened thin FGM cylindrical panels on elastic foundations. *Thin-Walled Structures*, **96**, (2015), pp. 155–168. https://doi.org/10.1016/j.tws.2015.08.005.

[21] T. Q. Quan, P. Tran, N. D. Tuan, and N. D. Duc. Nonlinear dynamic analysis and vibration of shear deformable eccentrically stiffened S-FGM cylindrical panels with

metal–ceramic–metal layers resting on elastic foundations. *Composite Structures*, **126**, (2015), pp. 16–33. https://doi.org/10.1016/j.compstruct.2015.02.056.

[22] L. T. N. Trang and H. V. Tung. Thermomechanical nonlinear analysis of axially compressed carbon nanotube-reinforced composite cylindrical panels resting on elastic foundations with tangentially restrained edges. *Journal of Thermal Stresses*, **41**, (2018), pp. 418–438. https://doi.org/10.1080/01495739.2017.1409093.

[23] M. M. Keleshteri and J. Jelovica. Nonlinear vibration behavior of functionally graded porous cylindrical panels. *Composite Structures*, **239**, (2020). https://doi.org/10.1016/j.compstruct.2020.112028.

[24] H. Akbari, M. Azadi, and H. Fahham. Free vibration analysis of thick sandwich cylindrical panels with saturated FG-porous core. *Mechanics Based Design of Structures and Machines*, **50**, (2020), pp. 1268–1286. https://doi.org/10.1080/15397734.2020.1748051.

[25] V. M. Anh and N. D. Duc. Nonlinear vibration of porous funcationally graded cylindrical panel using Reddy's high order shear deformation. *VNU Journal of Science: Mathematics - Physics*, **35**, (2019). https://doi.org/10.25073/2588-1124/vnumap.4444.

[26] D. Q. Chan, P. V. Hoan, N. T. Trung, L. K. Hoa, and D. T. Huan. Nonlinear buckling and post-buckling of imperfect FG porous sandwich cylindrical panels subjected to axial loading under various boundary conditions. *Acta Mechanica*, **232**, (2021), pp. 1163–1179. https://doi.org/10.1007/s00707-020-02882-6.